Carbon, 1976, Vol. 14, pp. 19–22. Pergamon Press. Printed in Great Britain

FLOW EQUATIONS FOR GRAPHITE

J. P. HIRTH
Metallurgical Engineering Department, The Ohio State University, Columbus, OH 43201, U.S.A.

E. E. HUCKE
Department of Materials and Metallurgical Engineering, The University of Michigan, Ann Arbor, MI 48104, U.S.A.

and

R. L. COBLE
Materials Science Department, Massachusetts Institute of Technology, Cambridge, MA 02139, U.S.A.

(*Received* 16 *April* 1975)

Abstract—In analyzing erosion of graphite at high strain rate ($\sim 10^7$ sec $^{-1}$) and temperature ($\sim$4000°C), it is necessary to have some approximation for the constitutive equation. Data for graphite from static and low strain rate experiments were successfully correlated using the equation $\dot{\epsilon}kT/DbG = C'(\sigma/G)^n$ which describes the flow of many metals and crystalline ceramics. Solution of the above equation for several specific cases of interest in hypersonic rain erosion at high temperature gives values for flow stress of from 2 to 10 kbar. Changes in temperature of about 500°C or strain rate by a factor 100 shift this value by more than 50%.

1. INTRODUCTION

Graphite is a candidate material for use at extremely high temperatures, and one important limitation is its erosion resistance for such applications as turbine components and nose cones. Of interest with respect to the theoretical understanding of the erosion problem is the appropriate constitutive equation for the substrate material under typical conditions. Among several possibilities is that of dislocation motion controlled deformation. Here, we investigate the possibility that such a flow behavior describes the deformation of ATJS graphite. This would both provide a possible rate equation for testing by computer codes in simulating erosion and would provide a basis for comparison with other constitutive equations to aid in deciding the actual deformation mechanisms of graphite under high velocity impact loading. An ancillary feature is a direct comparison of graphite flow behavior with that of metals and crystalline ceramic materials.

2. COMPARISON OF GRAPHITE WITH METAL AND CERAMIC CRYSTALS

It is of interest to investigate the possibility of calculating the flow of graphite under some extreme conditions typical of those encountered by graphite subject to erosion by hyper-sonic impact at high temperatures. Such conditions are typified by strain rates up to 10^6–10^7 sec^{-1} and temperature of 4000°C. Experimental measurements under these conditions are obviously difficult and the application of usual strength data should lead to appreciable error.

At elevated temperatures many metals and crystalline ceramics follow a rate equation of the form[1]

$$\dot{\epsilon} \propto \sigma^n f(T) \tag{1}$$

where $\dot{\epsilon}$ is strain rate, σ is resolved shear stress, and T is absolute temperature. Expressed in dimensionless form[1], guided by the fact that these materials deform by dislocation mechanisms involving vacancy diffusion, the equation assumes the form

$$\dot{\epsilon}kT/DbG = C'(\sigma/G)^n \tag{2}$$

where k is Boltzmann's constant, D is the self-diffusivity of the material in question, b is the dislocation Burgers vector, G the shear modulus and C' is a constant.

Figure 1 presents data which fit eqn (2), assembled from extensive results for a number of metals[1], plus data for magnesia[2], alumina[3] and several alkali halides[4]. A further expectation of the correlation in Fig. 1 is that materials with high stacking fault energies tend to lie on the low stress side of the range of observations, while those with low stacking fault energies lie on the high stress side. This expectation has been quantified[1, 4], but in view of the great uncertainties in values for stacking fault energies[5], the details are not presented here. On the basis of the qualitative correlation, however, graphite would be predicted to fit on the high stress side if it is deforming by a dislocation mechanism analogous to the crystalline materials. The stacking fault energy of graphite[6] is 0·7 erg/cm^2 vs a range from 15 erg/cm^2 (silver)[7] to 390 erg/cm^2 (LiF)[4, 8] to $\sim$1100 erg/cm^2 (tungsten)[5, 9].

Indeed, data for graphite[10] correlate very well with this prediction as indicated in Fig. 1. This data is primarily for ZTA graphite, but limited tests on ATJS graphite agree quite well with the data.

Both of these grades are fine grained, premium materials in terms of manufacturing defects and have a very well developed graphitic structure, which means their properties are extremely anisotropic on the atomic scale. In well developed graphite crystallites the crystal

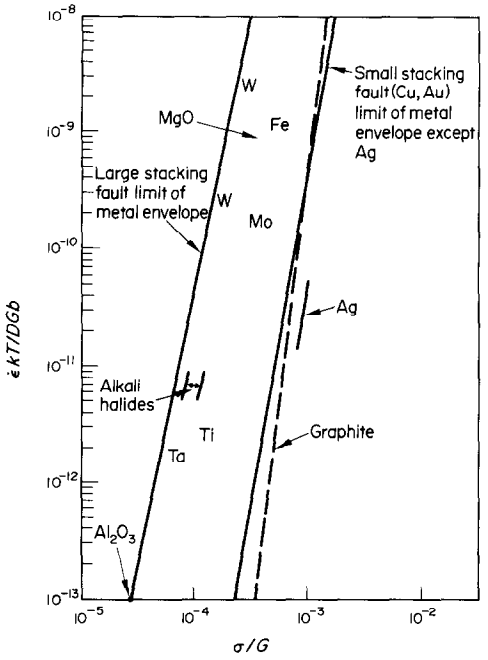

Fig. 1. Strain rate–stress correlation. $D = D_0 \exp(-Q/kT)$ exp PV/kT; $D_0 \simeq 1\,cm^2/sec$[11]; $Q = 277$ kcal/mole[10]; $G = C_{44}$ in basal plane $= 2{\cdot}3 \times 10^{10}$ dyn/cm^2[12]; $b = 2{\cdot}446 \times 10^{-8}$ cm for dislocation Burgers vector in basal plane[6]; $n = 8$[10]; P = hydrostatic component of stress tensor $= -(\sigma_1 + \sigma_2 + \sigma_3)/3$; $\bar{V}$ = activation volume for diffusion $\simeq$ atomic volume of carbon $= 5{\cdot}17 \times 10^{-24}$ cm^3; σ = maximum resolved shear stress $= (\sigma_1 - \sigma_3)/2$; σ_1, σ_2, σ_3 = principal stresses; ν = Poisson's ratio = 0·20[6].

structure is the well known hexagonal form[13]. These crystallites are on the order of 10^{-5} cm in diameter. It should be remembered that the macrostructure of artificial graphites is composed of grains, each made up of many crystallites. In a fine grained material like ATJS (grain size $\sim 15 \times 10^{-3}$ cm) there are many millions of crystallites per grain. As a result, there is always a substantial amount of micropore volume ranging in size from several hundred angstroms downwards. The ZTA grade is subjected to a hot deformation at very high temperatures during its manufacture. This process squeezes the grains together, rotating them so as to eliminate almost all the macropores, but giving a material that is highly anisotropic on both the micro and macro scales. This results in superior creep properties in directions parallel to the average basal plane orientation.

The carbon materials other than diamond all have varying amounts and distributions of voids, which are really more like built in cracks due to the inherent space filling limitations of a multigrained layered structure. It is therefore very easy to see how the mechanical property measurements are dominated by the manner in which an external load opens or closes up the spaces. The macroscopic strains may be largely made up of crack opening displacement which may be largely reversible. Such recovery of creep strain has long been noted in graphites. Recovery of compressive strain under a hardness test is also well known. Tensile creep data vary with ϕ, the angle between the axial load-force direction and the mean crystallographic c-axis orientation of the graphite. For $\phi = 0°$, tensile creep rates are a factor of 10^5 larger than compressive creep. This may be visualized as slowly opening the microcracks and extending them into one another. Compression, on the other hand, would tend to close these voids as well as the macropores so as to finally force deformation to take place within the crystallites. This picture would predict the observed coincidence of tensile and compressive creep for $\phi = 90°$, where relatively little of the easy crack opening displacement could occur.

The very high compressive stresses produced under an impacting projectile would initially close the void space. Further deformation would require some sort of atomic mobility. For this reason the correlation of Fig. 1 is based on steady state creep data at 2500°C, with compressive stresses of 2000–8000 psi, and strains $\geq 0{\cdot}10$.

One important implication of the correlation in Fig. 1 is that the graphite deforms at steady state in compression by dislocation motion, since it follows the same rate law as metals and crystalline ceramics which so deform.

3. CONSTITUTIVE EQUATION FOR GRAPHITE FLOW

We consider five explicit cases. In all cases, uniaxial strain ϵ_3 is assumed, corresponding to impact of a semi-infinite plate in the x_3 direction, so $\sigma_1 = \sigma_2 \neq \sigma_3$. The best guess at typical conditions is $T = 4000$°C, $\dot{\epsilon} = 10^6$ sec^{-1} as a near maximum imposed strain rate, Case A. Cases B, $T = 3500$°C and C, $T = 2500$°C, both with $\dot{\epsilon} = 10^6$ were selected to show expected variation with temperature. Case D, $T = 4000$°C, $\dot{\epsilon} = 10^7$ sec^{-1} was selected to indicate variation with strain rate. Finally, Case E with an "apparent" artificial modulus "G" = 100G was selected to show a possible equation for prismatic dislocations with a concordant much higher shear modulus C_{55}. For convenience, eqn (2) is recast in the form

$$\sigma/G = C(\dot{\epsilon}kT/DGb)^{1/8} \tag{3}$$

C was computed from the data in Ref. [10] and Fig. 1 to be 0·0148. The explicit equations for the various cases then assume the form

$$\pm(\sigma_1 - \sigma_3) = a \exp[C(2\sigma_1 + \sigma_3)] \tag{4}$$

with the parameters as given in Table 1.

Table 1. Data for various cases of eqn (4)

CASE	A	B	C	D	E
a	3.15	5.32	33.5	4.20	3.15
b	-3.53×10^{-4}	-4.00×10^{-4}	-5.65×10^{-4}	-3.53×10^{-4}	-3.53×10^{-4}
T, °C	4000	3500	2500	4000	4000
$\dot{\epsilon}$, sec^{-1}	10^6	10^6	10^6	10^7	10^6

Table 2. Data for five solutions of eqn (4). (+) and (−) correspond to the two solutions for each case. Stresses are given in kbars

	A		B		C		D		E	
σ_1	$(+)\sigma_3$	$(-)\sigma_3$	$(+)\sigma_3$	$(-)\sigma_3$	$(+)\sigma_3$	$(-)\sigma_3$	$(+)\sigma_3$	$(-)\sigma_3$	$(+)\sigma_3$	$(-)\sigma_3$
0.0	3.15	-3.16	5.31	-5.33	32.90	-34.17	4.19	-4.21	315.07	-315.77
-10.00	-6.82	-13.19	-4.63	-15.40	23.45	-44.76	-5.76	-14.25	305.10	-325.80
-20.00	-16.78	-23.23	-14.56	-25.46	14.01	-55.37	-15.72	-24.30	295.13	-335.84
-30.00	-26.75	-33.26	-24.50	-35.53	4.58	-65.99	-25.67	-34.34	285.13	-345.87
-40.00	-36.71	-43.29	-34.43	-45.59	-4.84	-76.61	-35.63	-44.39	275.20	-355.90
-50.00	-46.68	-53.33	-44.36	-55.66	-14.25	-87.25	-45.58	-54.44	265.23	-365.94
-60.00	-56.64	-63.37	-54.30	-65.73	-23.65	-97.90	-55.53	-64.48	255.27	-375.97
-70.00	-66.61	-73.40	-64.23	-75.80	-33.04	-108.57	-65.48	-74.53	245.30	-386.00
-80.00	-76.57	-83.44	-74.16	-85.87	-42.43	-119.24	-75.44	-84.58	235.33	-396.04
-90.00	-86.53	-93.47	-84.09	-95.94	-51.80	-129.93	-85.39	-94.63	225.37	-406.07
-100.00	-96.50	-103.51	-94.02	-106.01	-61.16	-140.63	-95.34	-104.68	215.40	-416.10
-110.00	-106.46	-113.55	-103.94	-116.09	-70.51	-151.34	-105.29	-114.73	205.43	-426.14
-120.00	-116.42	-123.59	-113.87	-126.16	-79.85	-162.06	-115.24	-124.78	195.47	-436.17
-130.00	-126.38	-133.62	-123.80	-136.23	-89.18	-172.80	-125.19	-134.83	185.50	-446.20
-140.00	-136.35	-143.66	-133.72	-146.31	-98.50	-183.55	-135.14	-144.88	175.53	-456.24
-150.00	-146.31	-153.70	-143.65	-156.39	-107.80	-194.31	-145.09	-154.93	165.57	-466.27
-160.00	-156.27	-163.74	-153.57	-166.46	-117.10	-205.09	-155.03	-164.98	155.60	-476.31
-170.00	-166.23	-173.78	-163.49	-176.54	-126.38	-215.88	-164.98	-175.04	145.63	-486.34
-180.00	-176.19	-183.82	-173.41	-186.62	-135.66	-226.68	-174.93	-185.09	135.67	-496.37
-190.00	-186.15	-193.86	-183.34	-196.70	-144.92	-237.50	-184.87	-195.15	125.70	-506.41
-200.00	-196.11	-203.90	-193.26	-206.78	-154.17	-248.34	-194.82	-205.20	115.73	-516.44
-210.00	-206.07	-213.95	-203.17	-216.86	-163.40	-259.19	-204.76	-215.26	105.77	-526.47
-220.00	-216.02	-223.99	-213.09	-226.95	-172.63	-270.05	-214.71	-225.31	95.80	-536.51
-230.00	-225.98	-234.03	-223.01	-237.03	-181.84	-280.94	-224.65	-235.37	85.83	-546.54
-240.00	-235.94	-244.07	-232.92	-247.12	-191.04	-291.83	-234.59	-245.43	75.87	-556.57
-250.00	-245.90	-254.12	-242.84	-257.20	-200.22	-302.75	-244.54	-255.48	65.90	-566.61

The results of computer calculations of eqn (4) are presented in Table 2 as values of σ_3 for the two solutions of eqn (4) for given values of σ_1. The + or − in eqn (4) correspond to the respective solutions where $\sigma_1 > \sigma_3$ and $\sigma_1 < \sigma_3$.

Work by McClintock[14] on erosion indicates that other constitutive laws give values of $|\sigma_1 - \sigma_3|$ in the range roughly 2·3–10 kbar. The results in Table 2 show that the typical Case A gives results, $|\sigma_1 - \sigma_3| \sim 3{\cdot}2$ kbar, very close to the lower band of these other equations. Comparisons with the other cases show that changes in temperature of 500°C or changes in strain rate by a factor of 10^2 can shift the value of $|\sigma_1 - \sigma_3|$ by more than 50%. Hence, the typical constitutive equation for the present flow case gives results of the order of the other possible constitutive equations; moreover, moderate changes in the typical parameters can shift the results to the lower bound of the other possibilities.

Gilman[15] has discussed both empirical and theoretical evidence to support a relation between the hardness, H, and the dynamic compressive yield stress, Y, for brittle materials. The empirical relation is

$$H = 2{\cdot}1Y. \tag{5}$$

Gilman calculates $H = 1{\cdot}8Y$ for silicon. In a very recent paper Oku and Eto[16] show data for a large number of graphites that are in remarkable agreement with eqn (5). Their correlation between compressive strength and Vickers hardness yields

$$H = 2{\cdot}27\sigma_c. \tag{6}$$

Using Gilman's relationship for calculating hardness from glide plane stiffness, G_{gp},

$$H = 0{\cdot}167G_{gp} \tag{7}$$

yields, with $C_{44} = G_{gp} = 2{\cdot}3 \times 10^{10}$ dyn/cm^2, $H = 39$ kg/mm^2.

Kegley and Leslie[17] measured the Knoop indentation hardness to be 34 for penetrating pyrolytic graphite sheet with the long axis of the indentor parallel to the layer structure. This result indicates that the low temperature modest strain rate compressive deformation of graphite can be calculated with the ordinary notions of plastic deformation. Using the calculated hardness together with eqn (5) gives

$$Y = 1{\cdot}8 \text{ kbar}$$

which compares well with the deductions from the correlation of Fig. 1 at high temperatures and high strain rate. It is interesting to note that the hardness for a knoop indentor forced into the layer structure with its long axis in the "C" direction is about 100 kg/mm^2 which would give $Y = 4{\cdot}6$ kbar, while for a lamellar pyrolytic carbon with a layer structure, but not necessarily with graphite stacking regularity, the average Diamond Pyramid Hardness was ~200 kg/mm^2 which corresponds to $Y \simeq 9{\cdot}2$ kbar. It is difficult to predict whether the highly amorphous forms of carbon could be treated in the same ways.

Since Drucker[18] has shown the relation of compressive strength to erosion resistance, it would be extremely valuable to have some simple method of estimating this property at the conditions of stress, strain rate, and temperature of interest.

The preliminary results presented here indicate that at least for highly graphitic materials the hardness might be used to estimate the compressive flow stress and that corrections for temperature and strain rate might be applied on the basis of Fig. 1, and eqn (2).

Acknowledgement—This research was supported by the Advanced Research Projects Agency of the Department of Defense under Contract No. DAHC15-71-C-0253 with The University of Michigan.

REFERENCES

1. Mukherjee A. K., Bird J. A. and Dorn J. E., *Trans. Quart. ASM* **62**, 155 (1969).
2. Langdon T. G. and Pask J. A., *Acta Met.* **18**, 505 (1970).
3. Cannon W. and Sherby O. D., *J. Am. Ceramic Soc.* **56**, 157 (1973).
4. Mohamed F. A. and Langdon T. G., *J. Appl. Phys.* **45**, 1965 (1974).
5. Hirth J. P. and Lothe J., *Theory of Dislocations*, pp. 292, 344, 353, 733. McGraw-Hill, New York (1968).
6. Amelinckx S., Delavignette P. and Heerschap M., in *Chemistry and Physics of Carbon* (edited by P. L. Walker, Jr.), Vol. 1, p. 1. Marcel Dekker, New York (1965).
7. Jossang T., *Phil. Mag.* **13**, 657 (1967).
8. Fontaine G. and Haasen P., *Phys. Stat. Sol.* **31**, K67 (1969).
9. Teutonico L. J., *Phys. Stat. Sol.* **10**, 535 (1965); **14**, 457 (1966).
10. Zukas E. G. and Green W. V., *Carbon* **6**, 101 (1968).
11. Shewmon P. G., *Diffusion in Solids*. McGraw-Hill, New York (1963).
12. Bowman J. C. and Krumhansl J. A., *J. Phys. Chem. Solids* **6**, 367 (1958).
13. Mantell C. L., *Carbon and Graphite Handbook*, p. 9. Interscience, New York (1968).
14. McClintock F. A., in *ARPA Materials Research Council Report*. University of Michigan (1974).
15. Gilman J. J., in *ARPA Materials Research Council Report*. University of Michigan (1974).
16. Oku T. and Eto M., *Carbon* **12**, 477 (1974).
17. Kegley T. M. and Leslie W. C., *Nucleonics* **21**, 63 (1963).
18. Drucker D. C., in *ARPA Materials Research Council Report*. University of Michigan (1974).